

Shin Seung Kak (Orcid ID: 0000-0002-5120-5300)

Exogenous 8-hydroxydeoxyguanosine ameliorates liver fibrosis through the inhibition of Rac1-NADPH oxidase signaling

Running Head: Exogenous 8-hydroxydeoxyguanosine in liver fibrosis

Seung Kak Shin,^{*} Kyung-Ok Kim,[†] Se-Hee Kim,[†] Oh Sang Kwon,^{*} Cheol Soo Choi,^{*,‡} Sung Hwan Jeong,^{*} Yun Soo Kim,^{*} Ju Hyun Kim,^{*} Myung-Hee Chung^{‡,§}

^{*}Department of Internal medicine, Gil Medical Center, Gachon University College of Medicine,

[†]Gachon Medical Research Institute, Gachon University Gil Medical Center, [‡]Lee Gil Ya

Cancer and Diabetes Institute, Gachon University, [§]Gachon Advanced Institute for Health

Sciences & Technology, Gachon University, Incheon, Republic of Korea

Correspondence:

Oh Sang Kwon, MD, PhD

Division of Gastroenterology and Hepatology, Department of Internal

This article has been accepted for publication and undergone full peer review but has not been through the copyediting, typesetting, pagination and proofreading process which may lead to differences between this version and the Version of Record. Please cite this article as doi: 10.1111/jgh.14979

Medicine, Gil Medical Center, Gachon University College of Medicine, 21, Namdong-daero
774 beon-gil, Namdong-gu, Incheon 21565, Republic of Korea

Tel: +82-32-460-3778, Fax: +82-322-460-3408

E-mail address: kos@gilhospital.com

Financial support:

This work has supported by the National Research Foundation of Korea (NRF) grant funded by the Korea government (MSIT) (No. NRF-2018R1C1B6006623), the Gachon University Gil Medical Center (Grant number: 2015-03-02), and Korean Association for the Study of the Liver-Liver Research Foundation of Korea.

Conflicts of Interest

The authors have no conflicts to disclosure.

Author contributions.

Seung Kak Shin wrote the manuscript and contributed to the analysis and interpretation of data. Oh Sang Kwon and Myung-Hee Chung contributed to the concept and design of the study. Seung Kak Shin, Oh Sang Kwon, Kyung-Ok Kim, and Se-Hee Kim performed the experiments. Cheol Soo Choi contributed to the analysis of blood sample. Oh Sang Kwon, Yun Soo Kim, Ju Hyun Kim, and Sung Hwan Jeong critically reviewed and approved the final draft; Ju Hyun Kim and Myung-Hee Chung supervised the study.

Abbreviations: 8-OHdG, 8-hydroxydeoxyguanosine; ACE, angiotensin-converting enzyme; AST, aspartate aminotransferase; ALT, alanine aminotransferase; BDL, bile duct ligation; CCK-8, cell counting kit-8; DCF-DA, 2',7'-dichlorofluorescein diacetate; ECM, extracellular matrix; GAPDH, glyceraldehyde 3-phosphate dehydrogenase; GAPs, GTPase activating proteins; GEFs, guanine nucleotide exchange factors; HSCs, Hepatic stellate cells; KCs, Kupffer cells; NOX, nicotinamide adenine dinucleotide phosphate (NADPH) oxidase; qRT-PCR, quantitative real-time polymerase chain reaction; ROS, reactive oxygen species; SECs, sinusoidal endothelial cells; SMA, smooth muscle actin; TGF- β , transforming growth factor- β ; TIMP-1, tissue inhibitor of metalloproteinase-1

Abstract

Background and Aim: Exogenous 8-hydroxydeoxyguanosine (8-OHdG) was suggested as an inhibitor of Rac1 and NADPH oxidase (NOX). The aim of this study was to evaluate the effects of the exogenous 8-OHdG on hepatic fibrogenesis in vitro and in vivo model of liver fibrosis.

Methods: Adult Sprague-Dawley rats were allocated to sham-operated rats (n=7), rats underwent bile duct ligation (BDL) (n=6), and BDL rats treated with 8-OHdG (60 mg/kg/day by gavage, n=6). All rats were sacrificed on day 21. Double immunofluorescence staining between either NOX1 or NOX2 and α -smooth muscle actin (SMA) in liver was performed. Hepatic fibrotic contents were assessed by hydroxyproline assay and quantified by Sirius red staining. In vitro, hepatic stellate cell (HSC) line LX-2 and HHStC cells were stimulated by angiotensin-II (10 μ M). The ROS production was measured by confocal microscopy. The expressions of NOX1, NOX2, α -SMA, transforming growth factor (TGF)- β 1, and collagen Ia

were analyzed by quantitative real-time polymerase chain reaction or immunoblotting.

Results: The 8-OHdG treatment in BDL rats reduced the NOX1 and NOX2 protein expression which overlapped with α -SMA compared to BDL rats. The 8-OHdG treatment in BDL rats significantly decreased the mRNA expression of NOX1, NOX2, α -SMA, TGF- β 1, and collagen I α , and fibrotic contents. Increases of reactive oxygen species (ROS) production, Rac1 activation, NOX1, NOX2, and fibronectin expression induced by angiotensin II in HSCs were attenuated by 8-OHdG.

Conclusions: Rac1 activation and NOX-derived ROS are implicated to liver fibrosis. The 8-OHdG ameliorates liver fibrosis through the inhibition of Rac1 activation and NOX-derived ROS.

Key Words: 8-hydroxydeoxyguanosine, liver fibrosis, NADPH oxidase, Rac1

Introduction

Liver fibrosis is characterized by excessive accumulation of extracellular matrix (ECM) proteins including collagen that occurs in most types of chronic liver diseases.¹ Hepatic stellate cells (HSCs) are the main ECM-producing cells in liver injuries regardless of the underlying etiology.² At this time, reactive oxygen species (ROS) are known as critical mediators of ECM production by activated HSCs.³

The stimulus for oxidative stress in the liver comes from multiple sources.⁴ Nicotinamide adenine dinucleotide phosphate (NADPH) oxidase (NOX) is a multicomponent enzyme complex that generates ROS in the course of liver damage.⁵ Recently, several studies have suggested that the critical role of NOX in the process of liver fibrosis.^{6,7} The NOX enzyme complex, especially NOX1 and NOX2 are composed of membrane and cytosolic components including Rac1.⁸

Rac, a small, GTP-binding protein in the Rho family, acts as an important component for NOX activity as well as cell proliferation and dynamic reorganization of the actin cytoskeleton.^{9, 10} Previous study demonstrated that sustained activation of Rac1 in HSCs perpetuates their activation and exacerbates liver fibrosis.¹¹ Therefore, reducing the Rac1 activity could be the important therapeutic targets for inhibition of hepatic fibrogenesis.

In an oxidative stress, the reaction of the hydroxyl radical with the DNA nucleoside deoxyguanosine results in the formation of endogenous 8-hydroxydeoxyguanosine (8-OHdG).¹² However, recent several reports have been suggested that exogenous 8-OHdG could reduce ROS production and proinflammatory mediators through the inhibition of Rac1 and NOX activation in inflammation- based diseases.¹³⁻¹⁶

The aim of this study is to confirm the possibilities of therapeutic implications of

exogenous 8-OHdG for liver fibrosis through the inhibition of Rac1-NOX signaling in vitro and in vivo model of liver fibrosis.

Methods

Liver fibrosis animal model. Male adult Sprague-Dawley rats (Orient Bio Inc., Korea) weighing 200–250 g were utilized in this study. The rats were maintained in a temperature-controlled room ($22 \pm 2^\circ\text{C}$), with a 12 hr light/dark cycle and a relative humidity of 40–60%, with ad libitum access to food and water. Rats were allocated to three groups: sham-operated rats (n=7), rats underwent bile duct ligation (BDL rats) (n=6), and BDL rats treated with 8-OHdG (60 mg/kg/day by gavage, n=6). For all surgical procedures, the rats were anesthetized by inhalation of 5 vol% isoflurane in 100% oxygen at a flow rate of 4 L/min for the induction and 2–3 vol% at 2 L/min for the maintenance. In the sham-operated group, a midline incision in the abdomen was made using sterile techniques and closed. BDL was performed using a standard technique.¹⁷ Each animal received a subcutaneous injection of 10 mg/kg ketoprofen for 1 day and 5 mg/kg gentamicin for 3 days, after surgery. All rats were sacrificed at 3 weeks after BDL. Serum samples were collected and stored at -80°C . Freshly dissected liver samples were fixed, processed, and paraffin-embedded for histologic examination. Liver tissues were snap-frozen in liquid nitrogen and stored at -80°C for further analysis. All animal experiments were approved by the Gachon University Institutional Animal Care and Use Committee (LCDI-2015-0009).

Reagents and materials. 8-OHdG was provided by Prof. Myung-Hee Chung of Gachon Advanced Institute for Health Sciences & Technology. Angiotensin II was purchased from

Sigma-Aldrich (St. Louis, MO) and 2',7'-dichlorofluorescein diacetate (DCF-DA) was purchased from Molecular Probes (Eugene, OR). The following antibodies for western blotting and immunohistochemistry were used: NOX1 (Novus Biologicals, Canada), NOX2 (Abcam, Cambridge, MA), α -smooth muscle actin (SMA) (Abcam, Cambridge, MA), Fibronectin (Santa Cruz Biotechnology, Santa Cruz, CA), GFP (Santa Cruz Biotechnology, Santa Cruz, CA) and Glyceraldehyde 3-phosphate dehydrogenase (GAPDH), (Santa Cruz Biotechnology, Santa Cruz, CA).

Serum biochemistry. Serum total bilirubin, alanine aminotransferase (ALT), and aspartate aminotransferase (AST) levels, alkaline phosphatase (ALP), and gamma glutamyl transferase (gamma-GT) were analyzed with an automatic analyzer (Cobas c111 System, Roche Diagnostics Ltd, Rotkreuz, Switzerland).

Double immunofluorescence. Double immunofluorescence staining on formalin-fixed paraffin-embedded sections was performed as described previously.⁷ Anti-NOX1 (red fluorescence), anti-NOX2 (red fluorescence), and α -SMA (green fluorescence) antibodies were used for double immunofluorescence. The nuclei were stained with propidium iodide (Invitrogen, Carlsbad, CA) and images were acquired using a Zeiss LSM 700 confocal microscope.

Hepatic hydroxyproline content. Hepatic hydroxyproline contents were quantified according to the manufacturer's protocol using a colorimetric hydroxyproline assay kit (Biovision, Mountview, CA). Liver tissue (10 mg) was incubated with 100 μ L of 12 N HCl for 3 hrs at

120°C. The hydrolyzed sample (10 µL) was transferred to a 96-well plate and allowed to dry. Chloramine-T (100 µL) was added to each well and the plate was incubated at 60°C for 90 min. The absorbance at 560 nm was recorded using an EMax® microplate reader (Molecular Devices, Sunnyvale, CA) and the concentrations were calculated based on a standard curve.

Histologic evaluation. Three-micrometer-thick sections obtained from the paraffin-embedded livers were stained with hematoxylin and eosin (H&E) solution for the evaluation of structural changes. Paraffin-embedded tissue sections were also stained with picosirius red (Sigma-Aldrich, St. Louis, MO) and counterstained with fast green (Sigma-Aldrich, St. Louis, MO) using previously published methods for quantifying the liver fibrosis content.¹⁸ Histological images of each sample were analyzed from six random 100× fields using Image J software (NIH, USA), and the percentage of red-stained area, which is a marker for collagen content, was measured. The data were pooled to determine the mean.

Cell culture. LX-2 cells, an immortalized human HSC line, were kindly provided by Prof. Ja June Jang of Department of Pathology, Seoul National University College of Medicine, and HepG2 cells were obtained from the Korean Cell Line Bank (Seoul, South Korea). Cells were cultured in DMEM medium (Hyclon, NY) supplemented with 2% fetal bovine serum (GIBCO, Grand Island, NY) and 1% antibiotic-antimycotic in a humidified 5% CO₂ atmosphere. The primary human hepatic stellate cells (HHStC, ScienCell Research Laboratories, CA) isolated from the human liver were cultured in stellate cell medium (ScienCell Research Laboratories, CA) supplemented with 2% fetal bovine serum and 1% penicillin-streptomycin in a humidified 5% CO₂ atmosphere.

Cell viability assay. HepG2, LX-2 and HHSteC cells were incubated for 72 hrs in medium with 8-OHdG at a range of concentrations (0, 50, 100, 250, and 500 $\mu\text{g}/\text{mL}$), respectively, and the cell viability was evaluated using the Cell Counting Kit (CCK)-8 (CK04-1000; Dojindo, Mashiki-machi, Japan).

DNA transfection. The following plasmids for overexpression were used: pCDNA3-EGFP-Rac1-WT (wild type, plasmid #12980, Addgene, Cambridge, MA) and pCDNA3-EGFP-Rac1-Q61L (constitutively active Rac1, plasmid #12981, Addgene, Cambridge, MA). LX-2 cells were transiently transfected using TransIT-X2[®] System in vitro DNA transfection reagent (Mirus Bio, Madison, WI) according to the manufacturer's protocol. Overexpression was confirmed by fluorescence analyses or western blot analyses with anti-GFP antibody.

Analysis of reactive oxygen species. Levels of ROS were detected using DCF-DA, which measures the production of cellular ROS such as hydrogen peroxide. LX-2 and HHSteC cells were pretreated with 8-OHdG (100 $\mu\text{g}/\text{mL}$) for 2hrs, and stimulated with 10 μM angiotensin-II. Cells were incubated with 25 μM DCF-DA in the dark for 30 min. DCF fluorescence was detected by confocal microscopy.

Rac1 activation assay. Rac1 activity was analyzed by determining the amount of GTP-bound Rac1 pulled down by interacting with GST-PAK-PBD (p21 activated kinase-protein binding domain) using the Rac1 activation assay kit (Cytoskeleton, Denver, CO), according to the manufacturer's instructions. LX-2 and HHSteC cells were pretreated with 8-OHdG for 2 hrs,

and then stimulated with 10 μ M angiotensin II for 5 min.

Quantitative reverse transcription PCR. Total RNA from frozen liver tissue was extracted using the RNeasy Mini Kit (Qiagen, Hilden, Germany) according to the manufacturer's standard protocol. Frozen liver tissues (10 mg) were disrupted in Buffer RLT (Qiagen, Hilden, Germany) and homogenized. The extracted RNA was eluted in 50 μ l of RNase-free water and stored at -80°C . Reverse transcription was carried out with the high-capacity cDNA reverse transcription kit (Applied Biosystems, Foster City, CA) for 15 min at 42°C with 1 μ g template RNA in a final volume of 20 μ l using the Quantitect RT kit (Qiagen Hilden, Germany) following the manufacturer's recommendations. The quantitative real-time polymerase chain reaction (qRT-PCR) was performed in the Bio-Rad CFX96 real-time PCR detection system (Bio-Rad, Hercules, CA), using the SYBR Premix Ex Taq II kit (Takara Biotechnology, Kyoto, Japan). Primers for specific genes are listed in Table S1. GAPDH was used as a reference for normalizing data.

Western blot. Harvested LX-2 cells, HHStcC cells and rat liver tissue were lysed in cold RIPA lysis buffer (0.5 M Tris-HCl, pH 7.4, 1.5 M NaCl, 2.5% deoxycholic acid, 10% NP-40, and 10 mM EDTA) containing protease and phosphatase inhibitors (GenDEPOT, San Jose, CA). Cell lysates were subjected to SDS-PAGE and then transferred to a nitrocellulose membrane. After blocking in 5% bovine serum albumin, the membrane was probed with anti-NOX1, anti-NOX2, anti- α -SMA and anti-fibronectin, followed by incubation with a secondary antibody conjugated to horseradish peroxidase. Then the membranes stripped and reprobed with an anti-GAPDH, anti- β -actin or α -tubulin antibody.

Statistical analysis. The data are presented as mean \pm standard deviation (SD). Statistical significance of the difference between experimental groups was assessed using the two-tailed Student's t-test, with a $P < 0.05$ considered to be statistically significant.

Results

Effects of 8-OHdG on fibrosis contents in BDL rat model. H&E staining of the liver tissue in BDL rats showed a marked bile duct proliferation and periportal inflammation. The 8-OHdG decreased the bile duct proliferation and periportal inflammation on H&E staining of the liver tissue (Fig. 1a). After Sirius red staining, remarkable collagen accumulation was observed in BDL rats based on the hyperplasia of the lattice fibers and collagenous fibers in the portal area. The 8-OHdG significantly decreased the collagen accumulation measured by Sirius red staining in BDL rats (Fig. 1b). The collagen contents (%) in sham-operated rats, BDL rats, and BDL rats treated with 8-OHdG were 0.19 ± 0.03 , 5.11 ± 0.26 , and 2.04 ± 0.86 respectively. The fibrosis contents were significantly higher in BDL rats than those in sham-operated rats ($P < 0.01$), and these changes were significantly decreased by 8-OHdG treatment ($P < 0.01$, Fig. 1c). The hydroxyproline levels ($\mu\text{g/g}$ liver tissue) in sham-operated rats, BDL rats, and BDL rats treated with 8-OHdG were 311.5 ± 73.0 , 1110.3 ± 358.0 , and 620.6 ± 169.1 , respectively. The levels were significantly higher in BDL rats than those in sham-operated rats ($P < 0.01$). The 8-OHdG significantly reduced the hydroxyproline levels ($P < 0.05$, Fig. 1d).

Effects of 8-OHdG on Rac1 activity, HSC activation and fibrosis-related gene activation in BDL rat model. Rac1 activities were evaluated by Rac1-GTP pull down assay. GTP-bound

Rac1 was higher in BDL rats than that in sham-operated rats, and relative band densities of GTP-bound Rac1 were significantly decreased in BDL rats treated with 8-OHdG than in BDL rats ($P < 0.05$, Fig. 2a). The hepatic mRNA expressions of α -SMA were increased in BDL rats than those in sham-operated rats. The 8-OHdG significantly reduced the mRNA expressions of α -SMA (6.2- vs. 2.6-fold, $P < 0.05$). In addition, BDL rats showed higher levels of hepatic protein expressions of α -SMA compared with sham-operated rats, but the relative band densities of α -SMA were significantly decreased in BDL rats treated with 8-OHdG ($P < 0.05$) (Fig. 2b). The hepatic mRNA expressions of fibrosis-related genes including transforming growth factor (TGF)- β , tissue inhibitor of metalloproteinase (TIMP)-1, and collagen $\alpha 1$ (I) were increased in BDL rats than those in sham-operated rats. The 8-OHdG significantly reduced the mRNA expressions of TGF- $\beta 1$ (7.7- vs. 3.4-fold, $P < 0.01$), TIMP-1 (17.0- vs. 3.4-fold, $P < 0.05$), and collagen I α (25.7- vs. 9.0-fold, $P < 0.01$, Fig. 2c-e).

Effects of 8-OHdG on NOX1 and NOX2 expression in BDL rat model. Double immunofluorescence stainings between either NOX1 or NOX2 and α -SMA of HSC activation marker, respectively. Most of NOX1 and NOX2 expressions overlapped with α -SMA-positive HSCs in BDL rats. The NOX1 and NOX2 protein expressions in liver by immunofluorescence were increased in BDL rats compared with sham-operated rats. However, those were attenuated by 8-OHdG treatment (Fig. 3a,b). We investigated the changes of mRNA expressions of NOX1 and NOX2 after BDL. Expression of hepatic NOX1 and NOX2 mRNA levels were elevated in BDL rats than those in sham-operated rats. The 8-OHdG significantly reduced the mRNA expression of NOX1 (7.3- vs. 2.7-fold, $P < 0.05$) and NOX2 (10.5- vs. 3.9-fold, $P < 0.01$, Fig. 3c,d).

Effects of 8-OHdG on serum biochemistry in BDL rat model. The total bilirubin levels were significantly higher in the BDL rats (7.5 ± 3.2 mg/dL) and BDL rats treated with 8-OHdG (7.9 ± 1.8 mg/dL) than those in the sham-operated rats (0.1 ± 0.5 mg/dL) ($P < 0.01$). The ALP levels were significantly higher in the BDL rats (266.6 ± 69.6 U/L) and BDL rats treated with 8-OHdG (303.1 ± 59.3 U/L) than those in the sham-operated rats (137.2 ± 28.2 U/L, $P < 0.01$). The gamma-GT levels were higher in the BDL rats (76.2 ± 91.4 U/L) and BDL rats treated with 8-OHdG (32.9 ± 23.2 U/L) than in the sham-operated rats (2.3 ± 0.9 U/L). However, the total bilirubin, ALP, and gamma-GT levels were not different between the BDL rats and BDL rats treated with 8-OHdG. Similarly, the serum AST levels were also higher in the BDL rats (447.4 ± 104.2 U/L) and BDL rats treated with 8-OHdG (637.0 ± 221.8 U/L) than in the sham-operated rats (60.2 ± 9.9 U/L) ($P < 0.01$). The serum ALT levels were also higher in the BDL rats (71.9 ± 18.9 U/L) and BDL rats treated with 8-OHdG (119.8 ± 63.9 U/L) than those in the sham operated rats (34.3 ± 6.6 U/L) ($P < 0.01$). However, the serum AST and ALT levels were not different between the BDL rats and BDL rats treated with 8-OHdG (Fig. S1).

Cell viability. The CCK-8 assay demonstrated that no significant toxicity on both LX-2 cells and hepG2 cells was observed at 8-OHdG concentrations of up to 250 μ g/mL at 24, 48, and 72 hr, respectively. And the CCK-8 assay also demonstrated that no significant toxicity on HHStcC cells was observed at 8-OHdG concentrations of up to 100 μ g/mL at 24, 48, and 72 hr, respectively.

Effects of 8-OHdG on ROS in angiotensin II-treated LX-2 and HHStcC cells. To evaluate the antioxidant effects of 8-OHdG, ROS production was measured by confocal microscopy. DCF fluorescence intensities measured by confocal microscopy were higher in angiotensin II-

treated LX-2 and HHSteC cells than those in control cells, respectively. The increases of DCF fluorescence intensities in LX-2 and HHSteC cells treated with angiotensin II were attenuated by 100 µg/mL 8-OHdG treatment. The relative densities of DCFDA fluorescence normalized to control were elevated in angiotensin II-treated LX-2 cells. The 8-OHdG reduced the relative densities of DCFDA fluorescence (13.4- vs. 0.5-fold). The relative densities of DCFDA fluorescence normalized to control were also elevated in angiotensin II-treated HHSteC cells. The 8-OHdG reduced the relative densities of DCFDA fluorescence (11.8 vs. 2.8-fold, Fig. 4a,b).

Effects of 8-OHdG on Rac1 activity in angiotensin II-treated LX-2 and HHSteC cells. Rac1 activities were evaluated by Rac1-GTP pull down assay. GTP-bound Rac1 was markedly activated in angiotensin-II treated LX-2 cells. The relative band densities of GTP-bound Rac1 were significantly decreased by 8-OHdG treatment in angiotensin-II treated LX-2 cells ($P < 0.05$, Fig. 5a). GTP-bound Rac1 was also markedly activated in angiotensin-II treated HHSteC cells. The relative band densities of GTP-bound Rac1 were significantly decreased by 8-OHdG treatment in angiotensin-II treated HHSteC cells ($P < 0.05$, Fig. 5b).

Effects of 8-OHdG on NOX1, NOX2, and fibronectin expressions in angiotensin II-treated LX-2 and HHSteC cells. NOX1, NOX2, and fibronectin protein expressions were assessed by western blotting in angiotensin II-treated LX-2 and HHSteC cells. NOX2 and fibronectin protein expressions in angiotensin II-treated LX-2 cells were markedly increased. The 8-OHdG treatment significantly reduced the relative band densities of NOX2 and fibronectin in angiotensin II-treated LX-2 cells ($P < 0.01$, Fig. 6a). NOX1, NOX2 and fibronectin protein expressions in angiotensin II-treated HHSteC cells were increased. The 8-OHdG treatment

significantly reduced the relative band densities of NOX1 ($P < 0.05$), NOX2 ($P < 0.05$) and fibronectin ($P < 0.01$) in angiotensin II-treated HHStcC cells (Fig. 6b).

Effects of 8-OHdG on increased fibronectin expression by constitutively active Rac1 in LX-2 cells. To determine whether Rac1 activation plays an important role in the process of liver fibrosis, LX-2 cells were transiently transfected. The transfection efficiency was about 40%. Constitutively active Rac1-treated LX-2 cells compared with wild type demonstrated significantly higher expression of fibronectin protein. Angiotensin II promoted fibronectin expression in constitutively active Rac1-treated LX-2 cells compared to expression in wild type. However, 8-OHdG treatment reduced the relative band densities of fibronectin expression in angiotensin-induced transfected cells (Fig. 7).

Discussion

In various clinical and experimental conditions of liver fibrosis, a critical role of oxidative stress has been suggested.^{19,20} Recent evidences indicate that NOXs may contribute to ROS production during liver fibrosis, being important roles in HSC activation.^{21,22} Paik et al.⁷ demonstrated the roles of NOX1 and NOX2 in liver fibrosis, and both NOX1 and NOX2 can be expressed in HSCs. In vivo model of our study, we also found increases the expression of NOX1 and NOX2 in co-expression of α -SMA, a marker of HSC activation and the increased expression of NOX1 and NOX2 was decreased when 8-OHdG was administered. Previous studies suggest that the renin–angiotensin systems including angiotensin-converting enzyme (ACE) and AT1R, which mediates cell proliferation, migration, and cell contraction, are markedly upregulated in the fibrotic liver.^{23,24} Angiotensin I is converted to angiotensin II by

ACE, and angiotensin II mainly acts through NOX in the liver. Several experiments provide evidence that angiotensin II is able to induce ROS production via activating NOX in human activated HSCs.^{21,25} The results of our in vitro study demonstrated that the protein expressions of NOX1, NOX2 and ROS generation were increased in angiotensin-II treated HSC, and the increased expressions of NOX1, NOX2 and ROS generation were attenuated by 8-OHdG treatment. As a result, these findings suggest that 8-OHdG administration might suppress the HSC activity through the inhibition of NOX-derived ROS. Meanwhile, our study showed the significant changes of NOX1 protein expressions in angiotensin II-treated primary hepatic stellate cell line, but not in angiotensin II-treated LX-2 cells. Further experiments may be needed to investigate why expression of NOX1 was different according to cell line.

The small G protein Rac1 is a subunit of NOX complex including NOX1, NOX2 and NOX3. The Rac1 activity is turned on by guanine nucleotide exchange factors (GEFs) and is turned off by GTPase activating proteins (GAPs).²⁶ To activate NOX, especially NOX1 and NOX2 in liver tissue, the activation of Rac1 is required.⁵ Previously, Huh et al.¹³ demonstrated that exogenous 8-OHdG would bind to the Rac1-GEF complex and stabilize the ternary complex of Rac1-GEF-8-OHdG, and these mechanisms of 8-OHdG could lead to Rac1 inactivation and NOX inactivation. Our study also showed the increase of Rac1 activity in angiotensin-II treated HSC, and the attenuation of Rac1 activity by 8-OHdG treatment. These results suggest that the 8-OHdG administration could lead to inhibition of NOX-derived ROS through the Rac1 inhibition.

Fibrosis is characterized by excess deposition of a collagen-rich ECM and excess production of ECM, and increased activity of TIMP which prevents ECM degradation.² Activated HSCs express an intracellular microfilament protein, α -SMA. TGF- β is the most potent fibrogenic factor for ECM production.²⁷ In our study, 8-OHdG can ameliorate the

expression of α -SMA, TGF- β , TIMP-1 and collagen I α which result from BDL-induced oxidative stress. In addition, 8-OHdG can also attenuate the expression of fibronectin in angiotensin II-induced HSC. Choi et al.¹¹ demonstrated that Rac1-transgenic mice demonstrates that induction of Rac1 in HSCs enhances their activation during liver injury and exacerbates hepatic fibrosis. Our study also confirmed that the transient transfection of constitutively active Rac1 plasmid DNA into LX-2 cell induced an increase of fibronectin expression which acts as an important indicator of ECM accumulation. And 8-OHdG treatment attenuated the transient transfection of constitutively active Rac1 plasmid DNA into LX-2 cell induced an increase of fibronectin expression. These results suggest that Rac1 plays an important role in liver fibrosis process and 8-OHdG may has an anti-fibrotic effect through the inhibition of Rac1.

The surgical ligation of the common bile duct could lead to cholestasis and hepatic inflammation resulting in a strong fibrotic reaction.²⁸ When the serum biochemistry of the BDL rats and BDL rats treated with 8-OHdG was analyzed in our study, appropriate cholestasis and hepatic inflammation were identified. However, 8-OHdG administration has not been shown to improve liver enzyme and liver function. Although the detailed mechanisms are still not fully understood, it is known that bile duct ligation-induced bile acid accumulation is toxic, and induces hepatocyte apoptosis and necrosis.^{29,30} Previous study has shown that NOXs including NOX 1, 2, and 4 are involved in the process of bile acid-induced apoptosis.³¹ Although 8-OHdG might lead to inhibit NOX1 and NOX2 through the inhibition of Rac1 activity, it could not inhibit the apoptosis process through NOX4 because NOX4 works independently of Rac1. In addition, 8-OHdG might not inhibit the various pathways associated with bile acid-induced necrosis. For this reason, despite the inhibition of NOXs and Rac1 by 8-OHdG, the liver enzymes and liver function did not show improvement in BDL rat model. The effect of 8-OHdG in the BDL model may be more specific to anti-fibrotic activity by inhibiting activity

on hepatic stellate cells than protecting hepatocyte.

Because 8-OHdG is one of the predominant forms of free radical-induced lesions of DNA, the concerns about the possibility of cytotoxicity may be raised when 8-OHdG is administered exogenously. However, previous studies have suggested that the activity of deoxynucleotide kinase which converts the exogenously administered 8-OHdG into 8-hydroxy-dGTP which can be used as a substrate of DNA polymerase for nucleoside synthesis is so very low that exogenously administered 8-OHdG cannot reincorporate into genomic DNA, and is less likely to be cytotoxic.³²⁻³⁴ In our study, the cytotoxicity of 8-OHdG to hepatocytes and hepatic stellate cells was scarcely observed, but rather decreased the ROS of the activated cells.

In conclusion, Rac1-NOX signaling in HSCs was associated with the hepatic fibrogenic process. The exogenous 8-OHdG might ameliorate the liver fibrosis through the inhibition of Rac1 activation and NOX-derived ROS. Thus, 8-OHdG could be a potent anti-fibrotic agent in liver fibrosis.

Acknowledgements

LX-2 cells were kindly provided by Prof. Ja June Jang of Department of Pathology, Seoul National University College of Medicine. Prof. Jung-Hwan Yoon (Seoul National University College of Medicine), Prof. Jeong-Hoon Lee (Seoul National University College of Medicine), and Prof. Seung Yeon Ha (Gachon University College of Medicine) have made great contributions to this article.

References

- [1] Friedman SL. Liver fibrosis -- from bench to bedside. *J Hepatol.* 2003; **38 Suppl 1**: S38-53.
- [2] Bataller R, Brenner DA. Liver fibrosis. *J Clin Invest.* 2005; **115**: 209-18.
- [3] Gandhi CR. Oxidative Stress and Hepatic Stellate Cells: A PARADOXICAL RELATIONSHIP. *Trends Cell Mol Biol.* 2012; **7**: 1-10.
- [4] Parola M, Robino G. Oxidative stress-related molecules and liver fibrosis. *J Hepatol.* 2001; **35**: 297-306.
- [5] Paik YH, Kim J, Aoyama T, De Minicis S, Bataller R, Brenner DA. Role of NADPH oxidases in liver fibrosis. *Antioxid Redox Signal.* 2014; **20**: 2854-72.
- [6] Aoyama T, Paik YH, Watanabe S, *et al.* Nicotinamide adenine dinucleotide phosphate oxidase in experimental liver fibrosis: GKT137831 as a novel potential therapeutic agent. *Hepatology.* 2012; **56**: 2316-27.
- [7] Paik YH, Iwaisako K, Seki E, *et al.* The nicotinamide adenine dinucleotide phosphate oxidase (NOX) homologues NOX1 and NOX2/gp91(phox) mediate hepatic fibrosis in mice. *Hepatology.* 2011; **53**: 1730-41.
- [8] Santillo M, Colantuoni A, Mondola P, Guida B, Damiano S. NOX signaling in molecular cardiovascular mechanisms involved in the blood pressure homeostasis. *Front Physiol.* 2015; **6**: 194.
- [9] Allal C, Favre G, Couderc B, *et al.* RhoA prenylation is required for promotion of cell growth and transformation and cytoskeleton organization but not for induction of serum response element transcription. *J Biol Chem.* 2000; **275**: 31001-8.
- [10] Hodge RG, Ridley AJ. Regulating Rho GTPases and their regulators. *Nat Rev Mol Cell Biol.* 2016; **17**: 496-510.
- [11] Choi SS, Sicklick JK, Ma Q, *et al.* Sustained activation of Rac1 in hepatic stellate cells promotes liver injury and fibrosis in mice. *Hepatology.* 2006; **44**: 1267-77.
- [12] Kasai H. Analysis of a form of oxidative DNA damage, 8-hydroxy-2'-deoxyguanosine, as a marker of cellular oxidative stress during carcinogenesis. *Mutat Res.* 1997; **387**: 147-63.
- [13] Huh JY, Son DJ, Lee Y, *et al.* 8-Hydroxy-2-deoxyguanosine prevents plaque formation and inhibits vascular smooth muscle cell activation through Rac1 inactivation. *Free Radic Biol Med.* 2012; **53**: 109-21.
- [14] Ock CY, Hong KS, Choi KS, *et al.* A novel approach for stress-induced gastritis based on paradoxical anti-oxidative and anti-inflammatory action of exogenous 8-hydroxydeoxyguanosine. *Biochem Pharmacol.* 2011; **81**: 111-22.
- [15] Ock CY, Kim EH, Hong H, *et al.* Prevention of colitis-associated colorectal cancer with 8-hydroxydeoxyguanosine. *Cancer Prev Res (Phila).* 2011; **4**: 1507-21.
- [16] Huh JY, Jung I, Piao L, Ha H, Chung MH. 8-Hydroxy-2-deoxyguanosine ameliorates high-fat diet-induced insulin resistance and adipocyte dysfunction in mice. *Biochem Biophys Res Commun.* 2017; **491**: 890-6.
- [17] Kountouras J, Billing BH, Scheuer PJ. Prolonged bile duct obstruction: a new experimental model for cirrhosis in the rat. *Br J Exp Pathol.* 1984; **65**: 305-11.
- [18] Yang L, Chan CC, Kwon OS, *et al.* Regulation of peroxisome proliferator-activated receptor-gamma in liver fibrosis. *Am J Physiol Gastrointest Liver Physiol.* 2006; **291**: G902-11.
- [19] Pietrangelo A. Iron, oxidative stress and liver fibrogenesis. *J Hepatol.* 1998; **28 Suppl 1**: 8-13.
- [20] Poli G, Parola M. Oxidative damage and fibrogenesis. *Free Radic Biol Med.* 1997; **22**: 287-305.

- [21] Liang S, Kisseleva T, Brenner DA. The Role of NADPH Oxidases (NOXs) in Liver Fibrosis and the Activation of Myofibroblasts. *Front Physiol.* 2016; **7**: 17.
- [22] Lan T, Kisseleva T, Brenner DA. Deficiency of NOX1 or NOX4 Prevents Liver Inflammation and Fibrosis in Mice through Inhibition of Hepatic Stellate Cell Activation. *PLoS One.* 2015; **10**: e0129743.
- [23] Paizis G, Cooper ME, Schembri JM, Tikellis C, Burrell LM, Angus PW. Up-regulation of components of the renin-angiotensin system in the bile duct-ligated rat liver. *Gastroenterology.* 2002; **123**: 1667-76.
- [24] Yoshiji H, Kuriyama S, Yoshii J, *et al.* Angiotensin-II type 1 receptor interaction is a major regulator for liver fibrosis development in rats. *Hepatology.* 2001; **34**: 745-50.
- [25] Bataller R, Schwabe RF, Choi YH, *et al.* NADPH oxidase signal transduces angiotensin II in hepatic stellate cells and is critical in hepatic fibrosis. *J Clin Invest.* 2003; **112**: 1383-94.
- [26] Cherfils J, Chardin P. GEFs: structural basis for their activation of small GTP-binding proteins. *Trends Biochem Sci.* 1999; **24**: 306-11.
- [27] Liu Y, Wen XM, Lui EL, *et al.* Therapeutic targeting of the PDGF and TGF-beta-signaling pathways in hepatic stellate cells by PTK787/ZK22258. *Lab Invest.* 2009; **89**: 1152-60.
- [28] Tag CG, Sauer-Lehnen S, Weiskirchen S, *et al.* Bile duct ligation in mice: induction of inflammatory liver injury and fibrosis by obstructive cholestasis. *J Vis Exp.* 2015.
- [29] Faubion WA, Guicciardi ME, Miyoshi H, *et al.* Toxic bile salts induce rodent hepatocyte apoptosis via direct activation of Fas. *J Clin Invest.* 1999; **103**: 137-45.
- [30] Woolbright BL, Dorko K, Antoine DJ, *et al.* Bile acid-induced necrosis in primary human hepatocytes and in patients with obstructive cholestasis. *Toxicol Appl Pharmacol.* 2015; **283**: 168-77.
- [31] Reinehr R, Becker S, Keitel V, Eberle A, Grether-Beck S, Haussinger D. Bile salt-induced apoptosis involves NADPH oxidase isoform activation. *Gastroenterology.* 2005; **129**: 2009-31.
- [32] Kim JE, Chung MH. 8-Oxo-7,8-dihydro-2'-deoxyguanosine is not salvaged for DNA synthesis in human leukemic U937 cells. *Free Radic Res.* 2006; **40**: 461-6.
- [33] Kim JE, Hyun JW, Hayakawa H, Choi S, Choi J, Chung MH. Exogenous 8-oxo-dG is not utilized for nucleotide synthesis but enhances the accumulation of 8-oxo-Gua in DNA through error-prone DNA synthesis. *Mutat Res.* 2006; **596**: 128-36.
- [34] Ock CY, Kim EH, Choi DJ, Lee HJ, Hahm KB, Chung MH. 8-Hydroxydeoxyguanosine: not mere biomarker for oxidative stress, but remedy for oxidative stress-implicated gastrointestinal diseases. *World J Gastroenterol.* 2012; **18**: 302-8.

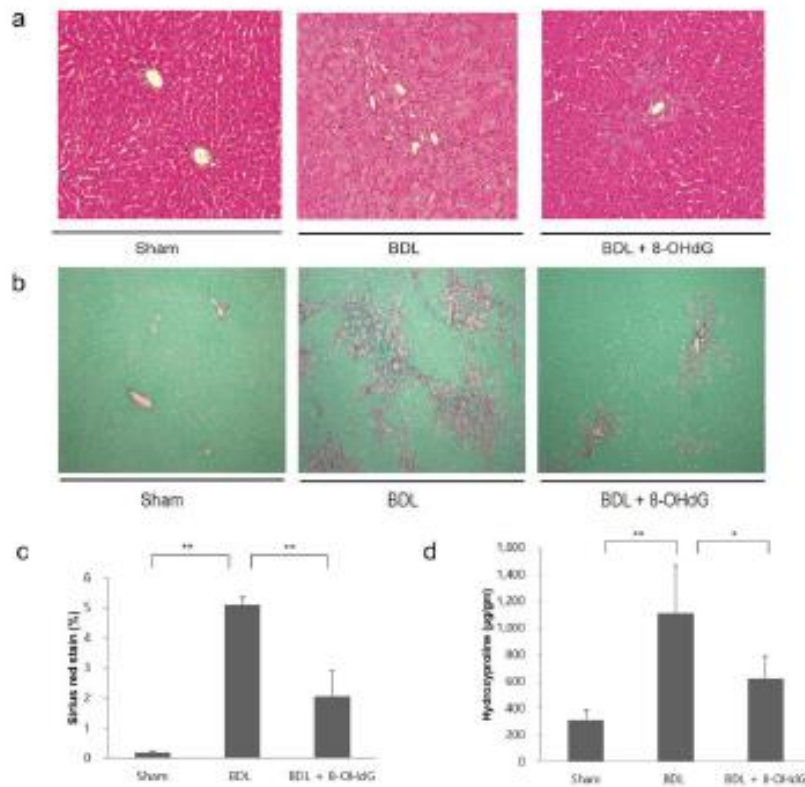


Figure 1 Effects of 8-OHdG on fibrosis contents in BDL rat model. (a) Representative images of H&E staining in Sham, BDL and BDL+8-OHdG rats were stained with the H&E solution to evaluate structural change (Original magnification $\times 100$). (b) Representative images of Sirius red staining in Sham, BDL and BDL+8-OHdG rats are shown (Original magnification $\times 100$). (c) Percentage of area stained was measured by image analysis from six random fields from each tissue section, and data were pooled to determine the mean. Data are expressed as mean \pm SD. (d) Fibrosis contents assessed by hydroxyproline assay in Sham, BDL and BDL+8-OHdG rats were measured. Data are representative of all animals from each group, and data are expressed as mean \pm SD. Sham, Sham-operated rats; BDL, rats underwent bile duct ligation; BDL+8-OHdG, BDL rats treated with 8-hydroxydeoxyguanosine; H&E, hematoxylin and eosin. * $P < 0.05$. ** $P < 0.01$.

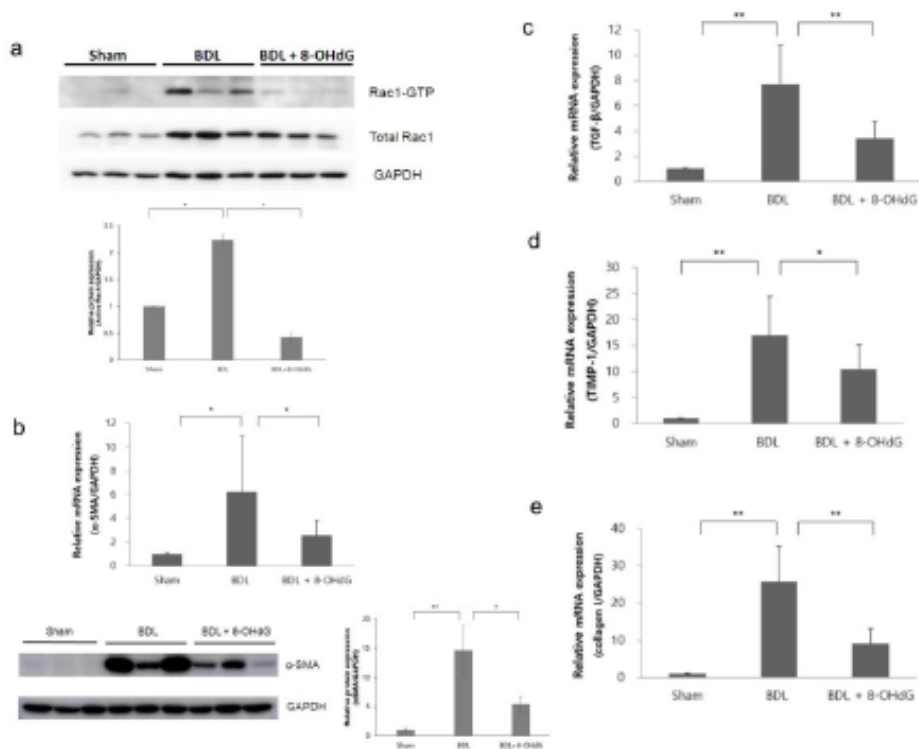


Figure 2 Effects of 8-OHdG on Rac1 activity, hepatic stellate cell activation, and fibrosis-related gene activation in BDL rat model. (a) The Rac1 activities were evaluated by pull down assay using PAK-PBD beads that specifically precipitate with Rac1-GTP, the active form of Rac1, which were then immunoblotted. GAPDH was used as a loading control. (b) Activation of hepatic stellate cells was assessed by qRT-PCR and western blotting for α-SMA. GAPDH was used as a loading control. Band densities were normalized against GAPDH and are shown as a ratio. Hepatic mRNA levels of (c) TGF-β, (d) TIMP-1, and (e) collagen Iα were measured by qRT-PCR. The relative band densities and relative mRNA expressions compared with the BDL rats were examined. GAPDH served as a loading control. Data are representative of all animals from each group, and data are expressed as mean ± SD. Sham, Sham-operated rats; BDL, rats underwent bile duct ligation; BDL+8-OHdG, BDL rats treated with 8-hydroxydeoxyguanosine. * $P < 0.05$. ** $P < 0.01$.

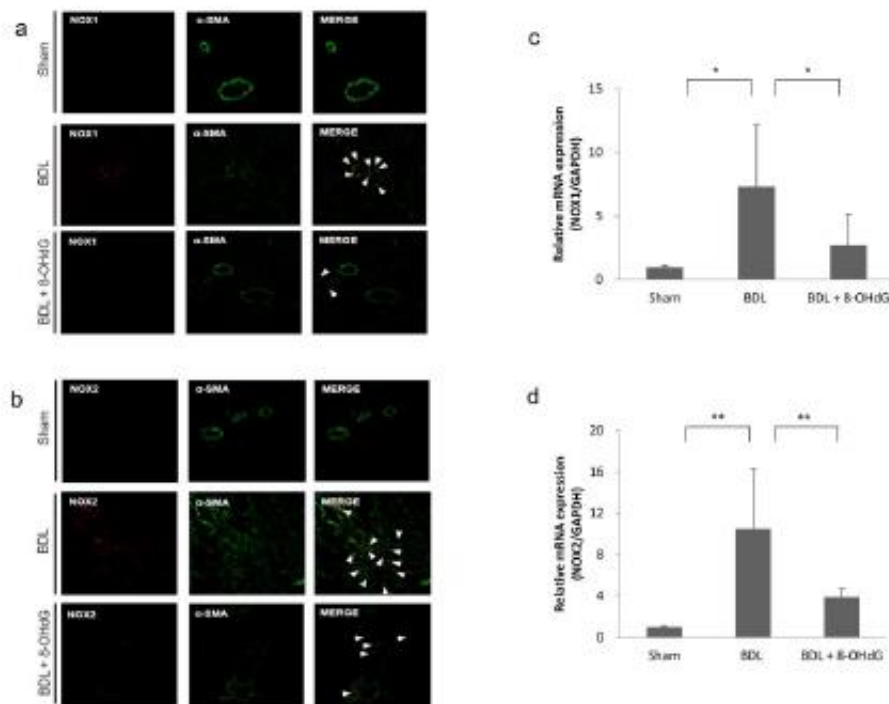


Figure 3 Effects of 8-OHdG on NOX1 and NOX2 expression of HSCs in BDL rat model. (a) Double immunofluorescence stainings for (a) NOX1 (red fluorescence) with α -SMA (green fluorescence) and (b) NOX2 (red fluorescence) with α -SMA (green fluorescence) were shown. Hepatic mRNA levels of (c) NOX1 and (d) NOX2 were measured after bile duct ligation using qRT-PCR. Data are representative of all animals from each group, and data are expressed as mean \pm SD. Sham, Sham-operated rats; BDL, rats underwent bile duct ligation; BDL+8-OHdG, BDL rats treated with 8-hydroxydeoxyguanosine. * $P < 0.05$, ** $P < 0.01$.

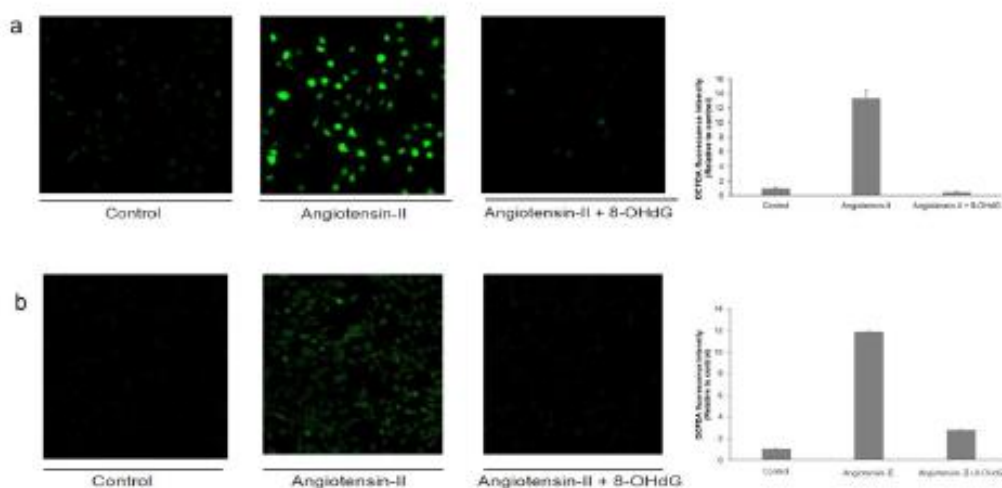


Figure 4 Effects of 8-OHdG on ROS production in angiotensin II-treated HSC. (a) LX-2 cells and (b) HHSteC cells were pretreated with 8-OHdG (100 $\mu\text{g}/\text{mL}$) for 2 hrs, and stimulated with 10 μM angiotensin-II for 2 min. Cells were incubated with 25 μM DCF-DA for 30 min. DCF fluorescence was detected by confocal microscopy. Quantity analysis of intensity of the DCFDA staining compared between groups. Data are expressed as the mean \pm SD of three independent experiments. 8-OHdG, 8-hydroxydeoxyguanosine; ROS, reactive oxygen species; DCF-DA, dichlorofluorescein diacetate.

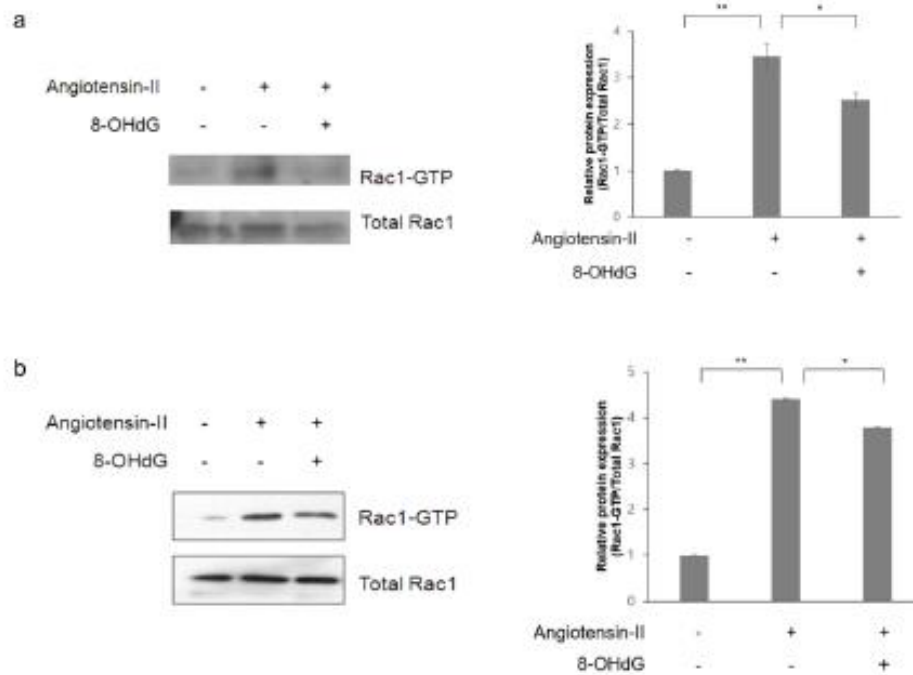


Figure 5 Effects of 8-OHdG on Rac1 activity in angiotensin II-treated HSC. (a) LX-2 cells and (b) HHStEC cells were pretreated with 8-OHdG (100 $\mu\text{g}/\text{mL}$) for 2 hrs, and stimulated with 10 μM angiotensin-II for 5 min. The Rac1 activities were evaluated by pull down assay using PAK-PBD beads that specifically precipitate with Rac1-GTP, the active form of Rac1, which were then immunoblotted. Amount of total Rac1 protein was determined and used as a loading control. Band densities were normalized against total Rac1 and are shown as a ratio. Data are expressed as the mean \pm SD of three independent experiments. 8-OHdG, 8-hydroxydeoxyguanosine.

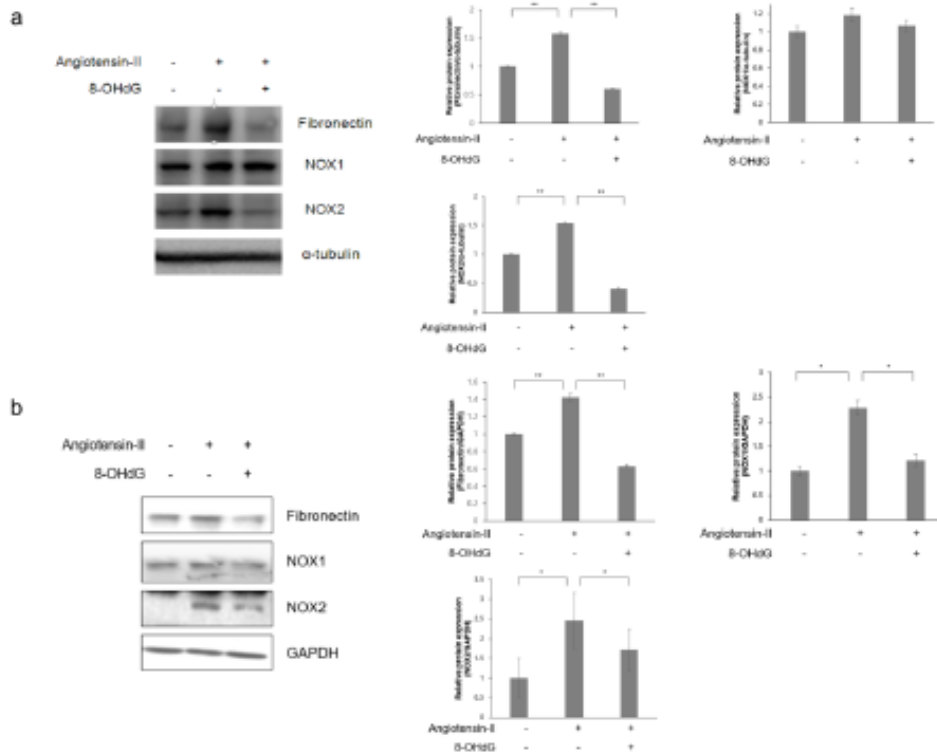


Figure 6 Effects of 8-OHdG on NOX1, NOX2, and fibronectin expression in angiotensin II-treated HSC. (a) LX-2 cells and (b) HHSteC cells were pretreated with 8-OHdG (100 μ g/mL) for 2 hrs, and stimulated with 10 μ M angiotensin-II for 48 hrs. The protein expression levels of NOX1, NOX2, fibronectin and α -tubulin were measured by western blot. α -tubulin was used as a loading control. Band densities were normalized against α -tubulin and are shown as a ratio. Data are expressed as the mean \pm SD of three independent experiments. NOX, NADPH oxidase; 8-OHdG, 8-hydroxydeoxyguanosine.

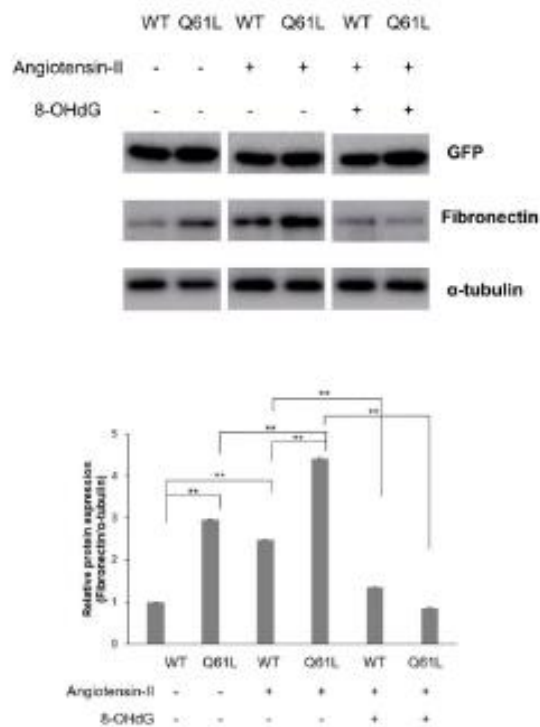


Figure 7 Effects of 8-OHdG on protein expression of fibronectin in angiotensin II induced LX-2 cells which were transfected with constitutively active Rac1 plasmid DNA. LX-2 cells were transiently transfected with wild type Rac1 (WT) or constitutively active Rac1 (Q61L). 24 hrs later, transfected cells were pretreated with 8-OHdG (100 μ g/mL) for 2 hrs, and stimulated with 10 μ M angiotensin-II for 24 hrs. The protein expression levels of GFP, fibronectin and α -tubulin were measured by western blot. α -tubulin was used as a loading control. Band densities were normalized against α -tubulin and are shown as a ratio. Data are expressed as the mean \pm SD of three independent experiments. 8-OHdG, 8-hydroxydeoxyguanosine; GFP, green fluorescent protein.